

Green synthesis of metal nanoparticles via natural extracts: the biogenic nanoparticle corona and its effects on reactivity

Kevin M. Metz,^a Stephanie E. Sanders,^a Joshua P. Pender,^a Michael R. Dix,^a David T. Hinds,^b

Susan J. Quinn,^b Andrew D. Ward,^c Paul Duffy,^d Ronan J. Cullen,^d and Paula E. Colavita^{d,e,}*

a - Department of Chemistry, Albion College, 611 E. Porter St., Albion, MI 49224, USA.

b - School of Chemistry, University College Dublin, Belfield, Dublin 4, Ireland

c - Central Laser Facility, Research Complex at Harwell, Science & Technology Facilities Council, Rutherford Appleton Laboratory, Didcot, Oxfordshire, OX11 0QX, UK

d - School of Chemistry, Trinity College Dublin, Dublin 2, Ireland.

e - Centre for Research on Adaptive Nanostructures and Nanodevices (CRANN), Trinity College Dublin, Dublin 2, Ireland

*Corresponding Author e-mail: colavitp@tcd.ie

Abstract

The optical and catalytic properties of metal nanoparticles have attracted significant attention for applications in a wide variety of fields, thus prompting interest in developing sustainable synthetic strategies that leverage the redox properties of natural compounds or extracts. Here, we investigate the surface chemistry of nanoparticles synthesized using coffee as a biogenic reductant. Building on our previously developed synthetic protocols for the preparation of silver and palladium nanoparticle/carbon composite microspheres a combination of thermogravimetric and spectroscopic methods were used to characterize the carbon microsphere and nanoparticle surfaces. Infrared reflectance spectroscopy and single particle surface enhanced Raman spectroscopy were used to characterize Pd and Ag metal surfaces, respectively, following synthesis. Strongly adsorbed organic layers were found to be present at metal nanoparticle surfaces after synthesis. The catalytic activity of Pd nanoparticles in hydrogenation reactions were leveraged to study the availability of surface sites, and coffee-synthesized nanomaterials were compared to commercial Pd-based hydrogenation catalysts. Our results demonstrate that biogenic adsorbates block catalytic surface sites and affect nanoparticle functionality. These findings highlight the need for careful analysis of surface chemistry as it relates to the specific applications of nanomaterials produced using greener or more sustainable methods.

Keywords: coffee, palladium, silver, nanoparticles, SERS, catalytic activity.

Introduction

The optical and catalytic properties of metal nanoparticles have attracted much attention for applications in a wide variety of fields, such as chemical sensing,^{1, 2} medicine,^{3, 4} and catalysis.⁵⁻¹⁰ The numerous applications of these nanomaterials has generated increased interest in new synthetic methods for their production. Moreover, increased interest in developing novel greener and/or more sustainable synthetic strategies has emerged recently. Sustainable approaches now include the use of microwave radiation,^{11, 12} plant extracts/biomass,¹³⁻¹⁹ bacterial templates,^{20, 21} and fungal systems²²⁻²⁴ as reducing agents.

The use of greener and more sustainable syntheses has many benefits. In particular, the use of natural products, fungi, or microbes as reducing agents decreases the requirements for chemicals such as sodium borohydrate, hydrogen gas or hydrazine, thus reducing waste and increasing the overall safety of the synthetic process. The use of natural products can also lead to capping groups that are biocompatible, circumventing the need for ligand exchange prior to biological applications.^{25, 26} Finally, the use of natural products can also represent a beneficial application of industrial byproducts or waste agricultural biomass, as has been shown in the case of the skin of wine grapes.¹⁶

The use of greener, more sustainable, or biogenic methods does not, however, guarantee the fabrication of nanomaterials with improved or even identical properties to those produced by traditional methods. The importance of natural compounds in green synthesis has been recently reviewed by Adil et al.,²⁵ who have pointed out that phytochemicals are likely responsible for nanoparticle size control through surface activity. However, they also emphasize that very little is known about the identity of such natural capping agents and about the effects, desirable or undesirable, they might have on nanoparticle functionality. It is becoming evident that as fabrication methods are altered, so too are the resulting surface chemical properties which are critical in determining nanoparticle functionality and applications. At least one study has shown varied toxicology from ZnO nanoparticles depending on the synthesis route used:²⁷ it was determined that the two methods used to produce ZnO nanoparticles

resulted in different surface chemical properties, which accounted for different degrees of toxicity.²⁷ As another example, we previously developed a method to make composites consisting of silver or palladium nanoparticles on carbon microspheres using coffee solution, i.e., a natural reducing agent.²⁸ While the application of these materials as catalyst`s was within the acceptable range for the reactions used, they performed at a lower level than anticipated. We hypothesized that the relatively low activity observed could be due to adsorbed natural compounds that form a surface blocking corona, therefore hindering catalytic activity. In this work we investigate the surface chemistry of nanoparticles synthesized using a natural reductant, and its impact on nanoparticle functionality. We have used synthetic protocols previously developed by us for the preparation of silver (Ag/CM) and palladium (Pd/CM) nanoparticle/carbon composite microspheres using coffee as reductant. Coffee solutions have a complex composition consisting of flavonoids, aliphatic/aromatic acids, lipids and melanoidins among others,²⁹ and together with leave infusions, are widely used as reductants in biogenic nanoparticle synthesis.^{13, 18} We characterized the microsphere surfaces by a combination of thermogravimetric and spectroscopic methods. In particular, the optical properties of silver were leveraged to directly probe nanoparticle adsorbates via single particle Surface Enhanced Raman Spectroscopy (SERS) of Ag/CM samples. We characterized the Pd surface via Infrared Reflectance Absorption Spectroscopy (IRRAS). We show that strongly adsorbed organic layers are present at the metal surface after synthesis. A study of the catalytic properties of Pd/CM materials demonstrates that these adlayers block surface sites such as those needed for metal-catalyzed reactions. Our findings highlight the need for careful analysis of surface chemistry of nanomaterials produced using greener or more sustainable methods for specific applications.

Experimental

Materials. Tin chloride dehydrate (96%, Fisher), palladium chloride (Fisher), silver nitrate (99%, Sigma), sodium hydroxide (97%, Sigma), potassium hydroxide (97%, Sigma), dichloroacetic acid (99%, Sigma), trifluoroacetic acid (TFA, 99%, Sigma), ammonia (28%, Romil), methyl-*trans*-cinnamate

(Sigma), potassium hexacyanoferrate(II) trihydrate ($K_4Fe(CN)_6$, Analar), 10% w/w Pd/carbon (Acros) and decaffeinated coffee powder (Sanka, or Nestle Decaffeinated) were used as received.

Synthesis of carbon and composite microspheres. Carbon microspheres (CMs) were synthesized using ultrasonic spray pyrolysis as reported previously.²⁸ Briefly, a 1.5 M solution of potassium dichloroacetate or sodium dichloroacetate was converted into droplets using a 1.7 MHz piezoelectric disk (APC International, Ltd.). An argon gas flow carried the droplets into a quartz tube furnace, where pyrolysis occurred at 710 °C. The resulting carbon microspheres were captured in a water bubbler, then isolated by filtration over a 0.45 μ m nylon filter and finally washed thoroughly with deionized water and ethanol. A three step process was used to create palladium nanoparticles on carbon microsphere composites (Pd/CM). CMs synthesized from potassium dichloroacetate, were sensitized in a solution of 0.050 M $SnCl_2$ and 0.070 M TFA in 50:50 water:methanol. Typically, a few milligrams of CMs were suspended in 10 mL of the tin solution using an ultrasonic bath and left to react at room temperature for 30 min. Following filtration and washing with water, sensitized CMs were activated in 3 mL of an acidified 0.005 M $PdCl_2$ solution (pH = 1), where they were left to react at room temperature for 30 min. A galvanic reaction between Sn^{2+} and Pd^{2+} occurs resulting in palladium nucleation on the CM surface. A coffee solution was prepared by adding 1.0 g Sanka coffee powder to 100 mL of boiling water, cooling to room temperature, and then filtering through a 0.45 μ m nylon membrane. 10 mL of the above coffee solution were added to activated CMs while still in the Pd^{2+} solution; the CM suspension was left to react for 30 min at room temperature yielding the Pd/CM composite particles. Pd/CMs were washed using at least 2 wash cycles consisting of collecting the composites by centrifugation then suspending the composites in fresh solvent. Typically one cycle was performed in deionized water and one in ethanol to remove palladium salts, excess nanoparticles, and coffee solution.

A similar process was used for the synthesis of silver nanoparticle/carbon microsphere composites (Ag/CMs), as previously reported.²⁸ The only difference were the use of sodium dichloroacetate as the precursor for CM synthesis, the use of 0.003 M $Ag(NH_3)_2^+$ instead of $PdCl_4^{2-}$, and the use of Nestle decaffeinated coffee as the reducing agent.

Characterization. Microanalysis of nanoparticle/CM composites was carried out using a Scanning Electron Microscope (SEM, Zeiss Ultra) equipped with an energy dispersive X-ray spectroscopy detector (EDS, Oxford Instruments); images were collected at 10 keV accelerating voltage using an in-lens secondary electron detector. Samples were prepared by drop casting of particle suspensions in methanol onto silicon wafers. Elemental analysis was performed using a standardless protocol provided with the EDS. Brunauer-Emmett-Teller (BET, Quantachrome Nova Station) analysis was used to determine the specific surface area of the carbon microspheres. Samples were pre-treated at 200 °C under vacuum for 24 h prior to analysis using nitrogen as the adsorbing gas. The specific surface area was calculated using a multi-point BET plot over relative pressures in the range of 0.08-0.3. Metal loadings were determined using thermogravimetric analysis (TGA, Perkin-Elmer Pyris 1) in air. Samples were held at 200 °C to desorb physisorbed solvents prior to initiating a 10 °C min⁻¹ heating ramp. At least 1 mg of well washed sample was used in all TGA measurements and masses were normalized to the sample weight at 200 °C. Bulk Raman spectroscopy was carried out on a microraman spectrometer (Renishaw 1000) equipped with a CCD detector and excitation at 457 nm. Fourier Transform Infrared Spectroscopy (FTIR) was carried out in Attenuated Total internal Reflectance mode (ATR-FTIR, Perkin Elmer), in external Reflectance-Absorbance mode (IRRAS, Bruker Tensor 27 with Veemax II accessory) and in transmittance mode using KBr pellets.

Combined Raman-optical tweezer studies of Ag/CM microspheres were carried out using a previously described custom-built setup.³⁰⁻³² The Raman tweezers apparatus consists of a CW Verdi V8 (Coherent) with laser beam wavelength of 532 nm, in combination with an Leica microscope equipped with a 60× NA 1.2 water immersion objective lens. For particle trapping and acquisition of Raman spectra, the laser was attenuated to a power of 2.2 mW, measured at the entrance aperture of the objective lens, yielding approximately 1.4 mW at the objective output. The Raman light scattered from the focal point was collimated by the objective lens and directed through a Semrock 532 nm razor-edge filter before refocussing onto the entrance slit of a spectrometer (SpectraPro-2500i, Acton Research Company) and detector (Spec-10:400B, Princeton Instruments); calibration of the spectrometer was performed using

liquid toluene as a standard and was accurate to 2 rel. cm^{-1} . All spectra were recorded at 1 s exposure; a CCD camera was used to allow observation of particles during measurements.

Catalytic Studies. The hydrogenation of methyl-*trans*-cinnamate was used as a model reaction to study the catalytic activity of Pd/CMs. The hydrogenation of methyl-*trans*-cinnamate was selected because it is a facile reaction that produces high yields in short times at room temperature.³³ In a typical reaction 1-2 mg of Pd/CM were added to 100 mg (1 mmol) of methyl-*trans*-cinnamate in 5 mL of ethanol in a 100 mL round bottom flask. The round bottom flask was twice evacuated and back filled with hydrogen gas. A hydrogen generator (Parker) was used to maintain a 1 atm/15 psi pressure of hydrogen gas for the duration of the reaction (30-120 min). The reaction solution was filtered through a 0.45 μM nylon membrane to remove the catalyst, and the products were isolated using rotary evaporation. The reaction products were identified and quantified using $^1\text{H-NMR}$. Control experiments were carried out using 6-8 mg of commercially available 10% w/w Pd/carbon.

Results and Discussion

Synthesis and characterization of nanoparticle/carbon composite microspheres

We used carbon microspheres (CMs) fabricated by ultrasonic spray pyrolysis (USP) as scaffolds for metal nanoparticle composites studied in this work.^{34, 35} Figure 1a shows an SEM image of a bare CM synthesized from potassium dichloroacetate precursor solution via USP. These CMs display a diameter of $1.7 \pm 0.5 \mu\text{m}$, with a size distribution as shown in Figure 1b, and an active surface area of $631 \text{ m}^2 \text{ g}^{-1}$, determined by BET analysis. Figure 1c shows a Raman spectrum of the CMs in Figure 1a; the spectrum displays peaks at 1364 and 1590 cm^{-1} which are characteristic of the D and G bands, respectively, of amorphous carbon.^{28, 36} Figure 1d shows the corresponding FTIR absorbance spectrum of CMs; the spectrum displays two broad peaks in the region $1800\text{-}1000 \text{ cm}^{-1}$ with maxima at 1591 and 1270 cm^{-1} .³⁰ The maximum at 1591 cm^{-1} can be assigned to the C—C stretching modes of graphitic structures and indicate that the precursor undergoes pyrolysis yielding a carbon scaffold,^{37, 38} in agreement with Raman results. The FTIR also shows a broad shoulder at 1700 cm^{-1} that can be assigned to C=O stretching

modes, likely due to the presence of surface carboxylic acid groups.^{30, 39} Carbon microspheres synthesized from a 1.5 M sodium dichloroacetate precursor have similar properties which have previously been discussed in detail.³⁰

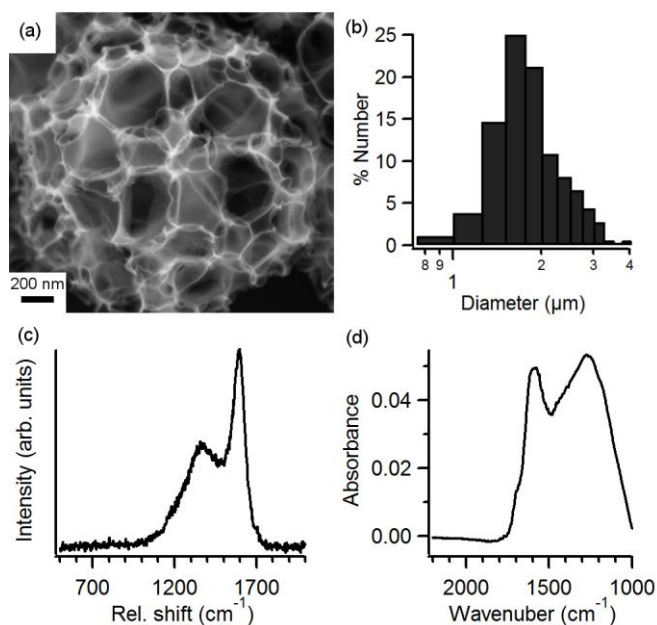
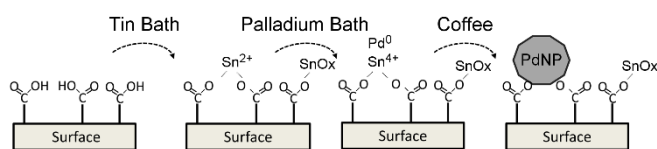


Figure 1. (a) SEM image of bare carbon microspheres synthesized from potassium dichloroacetate precursor solutions; (b) Size distribution of carbon microspheres; (c) Raman of carbon microspheres measured from the dry powder, excitation 457 nm; (d) FTIR absorbance spectrum of carbon microspheres.



Scheme 1. Synthesis protocol used for the preparation of Pd/CM materials.

We synthesized metal nanoparticles on CMs using a three-step method used previously and outlined in Scheme 1.²⁸ Briefly, CMs were first sensitized in a Sn^{2+} solution, then activated in a Pd^{2+} solution and finally immersed in a coffee solution yielding Pd/CM composite particles. Figure 2a, 2b and 2c show images of the carbon scaffold after each one of these steps, obtained via SEM. Following sensitization (Figure 2a) the CM walls change morphology, suggesting the presence of surface bound materials.

Previous studies on sensitization of carbon substrates using the same protocol show that Sn^{2+} adsorption leads to the formation of tin carboxylates at the carbon surface⁴⁰ and that this step is required for the formation of supported metal nanoparticles.²⁸ After activation in PdCl_4^{2-} solutions (Figure 2b) it is possible to distinguish the presence of small bright clusters, consistent with the formation of Pd^0 nanoparticles at the carbon surface via galvanic reaction between surface bound Sn^{2+} and the PdCl_4^{2-} complex. Composite particles obtained after this step are referred to, from hereon, as activated-Pd nanoparticles on carbon microspheres (aPd/CM). Addition of the coffee solution yields CMs that are densely decorated with nanoparticles that are approximately 20 nm in diameter, as shown in Figure 2c. Coffee solutions have been shown by us and other groups to act as effective reductants for the formation of palladium nanoparticles from palladium complexes in solution.^{14, 28} Here, the coffee was found to reduce palladium ions onto the surface-bound nucleation sites, resulting in the formation of Pd/CM composites. The composites were collected by centrifugation and washed multiple times by suspension in clean solvent followed by centrifugation. To test the role of coffee in Pd/CM synthesis and functionality, studies described in the following sections were performed with composites prepared both with (Pd/CM) and without addition of the coffee solution (aPd/CM).

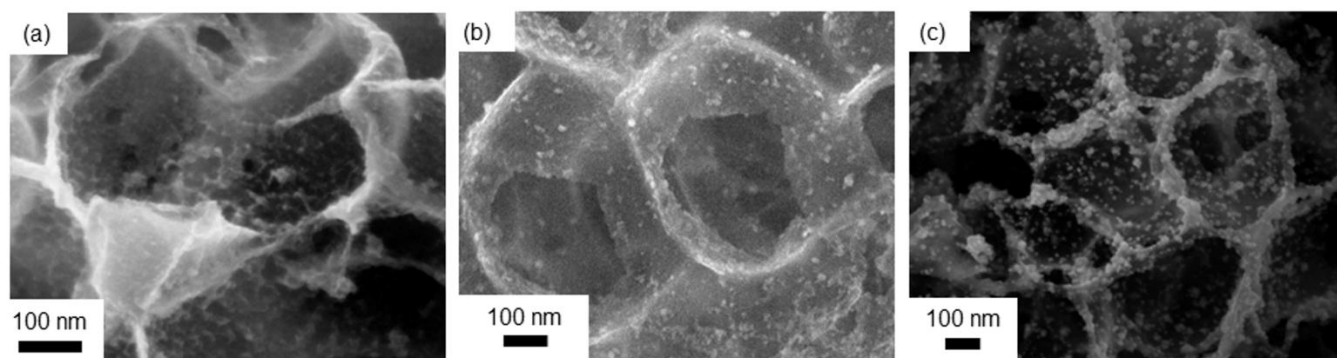


Figure 2. SEM image showing details of the carbon scaffold walls after (a) sensitization with Sn^{2+} , (b) activation with PdCl_4^{2-} and (c) coffee reduction.

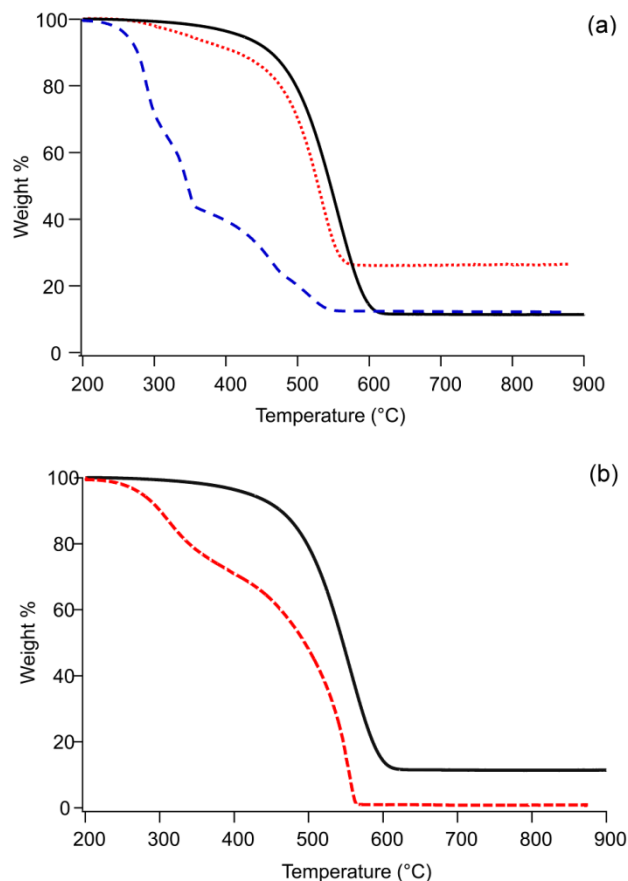


Figure 3. TGA curves obtained at $10\text{ }^{\circ}\text{C min}^{-1}$ in air for: (a) bare carbon microspheres (CM, black solid line), activated palladium on CM (aPd/CM, red dotted line) and palladium nanoparticles on carbon microspheres (Pd/CM, blue dashed line); (b) bare carbon microspheres (CM, black solid line) and carbon microspheres after incubation in coffee (red dashed line).

In order to characterize the loading and composition of Pd/CMs we carried out thermogravimetric analysis (TGA). Figure 3a shows TGA data obtained in air for bare CM, aPd/CM and Pd/CM samples over the temperature range 200-900 °C. Bare CMs show a single mass loss process over the 400-620 °C temperature range, with the greatest mass loss rate at 550 °C, which corresponds to the oxidation of the carbon scaffold. The curve for aPd/CM samples shows mass loss over the range of 300-575 °C, with the greatest oxidation rate occurring at 520 °C. Oxidation of aPd/CMs occurs at slightly lower temperatures than for bare CMs, which is consistent with the role of palladium in catalyzing the oxidation of graphitic carbon.^{28, 41} The curve for Pd/CM shows three distinct oxidation steps over the range of 225-550 °C; the

presence of multiple steps indicates that organic material, different from the graphitic carbon, undergoes oxidation at lower temperatures than the carbon scaffold. In order to understand the origin of this additional organic material we carried out TGA analysis on bare CM particles that had been soaked in coffee and washed (coffee/CM) following the same protocol as for Pd/CM composites; Figure 3b shows the TGA of coffee/CM samples compared to that of bare CMs. The coffee/CM curve displays a mass loss starting at 225 °C of approximately 28% that suggests that low temperature mass losses observed for Pd/CM samples may be attributed to combustion of organic compounds adsorbed from coffee.

Analysis of the residual masses at 850 °C from TGA curves, in combination with EDS analysis of particles, allowed for the determination of Pd/C metal loadings following a previously published approach.²⁸ The residual masses for aPd/CM and Pd/CM samples were $28.0 \pm 6\%$ and $12.2 \pm 0.4\%$, respectively; these masses are due to insoluble salts and oxides left after combustion of the carbon scaffold, tin sensitization and palladium activation and growth steps. The residual masses observed for bare CM and coffee/CM samples were $11.8 \pm 0.8\%$ and $1.3 \pm 0.4\%$, respectively; these arise only from the presence of inorganic salts/oxides left after combustion of carbon. The Pd:Sn atomic ratio was determined by EDS to be 20:80 and 25:75 for aPd/CM and Pd/CM, respectively. These results were used to calculate w/w% Pd/C from the mass residues by taking into account that tin is oxidized after completion of the TGA curve to SnO₂, while Pd must be present exclusively as Pd⁰ because its oxides decompose below 850°C.^{28, 42} After correction for the presence of residuals from the pyrolysis, the w/w% Pd/C of composites were calculated to be $2.3 \pm 0.8\%$ for aPd/CM and $2.0 \pm 0.1\%$ for Pd/CM. This result is surprising when considering that SEM images in Figure 2 indicate that more clusters are present on Pd/CM than on aPd/CM samples; therefore, it suggests that the amount of organic/carbon-rich material associated to the carbon scaffold is greater for Pd/CM than for aPd/CM particles, thus resulting in lower w/w% Pd/C values.

We have previously published a detailed report on the synthesis and characterization of Ag/CM composites, synthesized as described above.²⁸ Briefly, carbon microspheres synthesized using USP from a sodium dichloroacetate solution have an average diameter of $1.8 \pm 0.5 \mu\text{m}$ and a surface area of 473

$\text{m}^2 \text{g}^{-1}$. Individual Ag nanoparticles, synthesized with coffee on these supports and following a similar procedure as above, were ~ 25 nm in diameter, but were often present as aggregates of 100-200 nm in the composite material. The Ag/CM had a $(13.5 \pm 1.5)\%$ w/w metal loading, determined by TGA and EDS. Ag/CM materials were used in the following section to study the metal surface of nanoparticles after synthesis via Raman spectroscopy, by leveraging the surface enhancing optical properties of Ag nanoparticles.

Characterization of metal surfaces

In order to investigate the Pd interface we carried out IRRAS characterization of Pd thin films after exposure to coffee solutions used for nanoparticle deposition. Figure 4 shows an IRRAS spectrum of a Pd surface after exposure to coffee, obtained using a bare Pd substrate as the background sample; the spectrum of coffee powder obtained via ATR-FTIR is also reported for comparison. The spectrum displays prominent peaks at 2930 and 2875 cm^{-1} , which are characteristic of C—H stretching modes of aliphatic chains and are typically present in the infrared signature of coffee.^{39,43} A broad peak consisting of multiple contributions and with resolved maxima at 1670 and 1606 cm^{-1} is characteristic of carbonyl stretching modes and C—C stretching contributions from aromatic (chlorogenic) acids and caffeine.⁴³⁻⁴⁵ Finally, there are two additional smaller peaks at 1285 and 1090 cm^{-1} that fall in the region of C—O stretching modes and can be assigned to the presence of chlorogenic acids and saccharides.⁴⁴ A comparison of IRRAS data with the ATR-FTIR spectrum of coffee powder used for preparing reducing solutions suggests a good correspondence between compounds present in coffee and those found at the Pd surface, thus indicating that organic residues can bind to palladium surfaces following the washing procedure employed in this work.

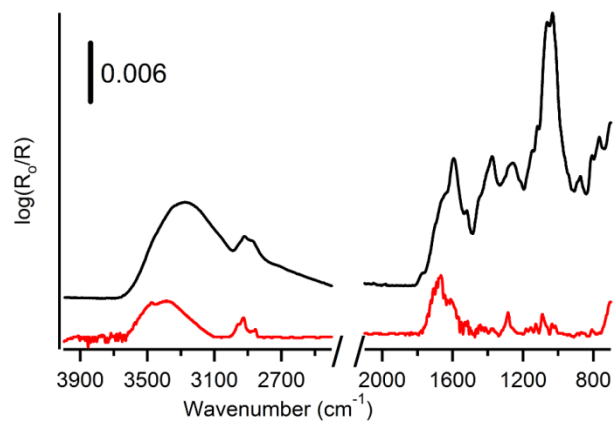


Figure 4. IRRAS spectrum of a Pd surface after exposure to coffee, obtained using a bare Pd substrate as the background sample (bottom, red trace) and ATR-FTIR spectrum of coffee powder (top black trace). Spectra were baseline corrected and offset for clarity; the coffee powder spectrum was multiplied by 0.1 to facilitate comparison.

To understand whether surface capping of metals with natural compounds is a general problem not restricted to Pd nanoparticles, we also investigated the surface of silver nanoparticles in Ag/CM composites synthesized via coffee reduction. In the case of carbon-supported Ag, we were able to leverage its surface enhancement properties in order to directly interrogate Ag/CM particles via Raman spectroscopy. Individual particles were optically trapped using a high numerical aperture objective and a 532 nm laser that also served for Raman excitation. Raman spectra were collected once every second during the particle residence time in the trap. Figure 5 shows examples of Raman spectra recorded for trapped particles, after subtraction of the carbon background Raman peaks (see Supporting Information); no peaks were observed when the laser was focused in the liquid bulk. Different peaks were observed for each particle, with the signature of organic compounds being clearly discernible in the fingerprint region for the majority of trapping events. The spectra in Figure 5 display signatures characteristic of esters ($1760\text{-}1730\text{ cm}^{-1}$), polyphenols and chlorogenic acids ($1660\text{-}1600\text{ cm}^{-1}$), coffee-specific diterpenes (1567 and 1480 cm^{-1}) and aliphatic groups (1450 , 1375 and 1263 cm^{-1}).⁴⁶⁻⁴⁸ Peaks were found to disappear within the time needed for recording ~ 2 spectra (2 s); this could be due to beam damage of coffee components during Raman, as previously reported,⁴⁶ or to heating effects of laser

illumination. To confirm that the observed peaks result from surface-enhanced Raman spectroscopy (SERS) of organics adsorbed onto Ag, we carried out control experiments using carbon particles incubated in coffee and subsequently rinsed, which did not yield spectra as the ones in Figure 5. Also, we carried out ligand exchange experiments using $K_4Fe(CN)_6$ solutions⁴⁹ which confirmed that the observed spectra originate from SERS of adsorbates at the Ag surface (see Supporting Information).

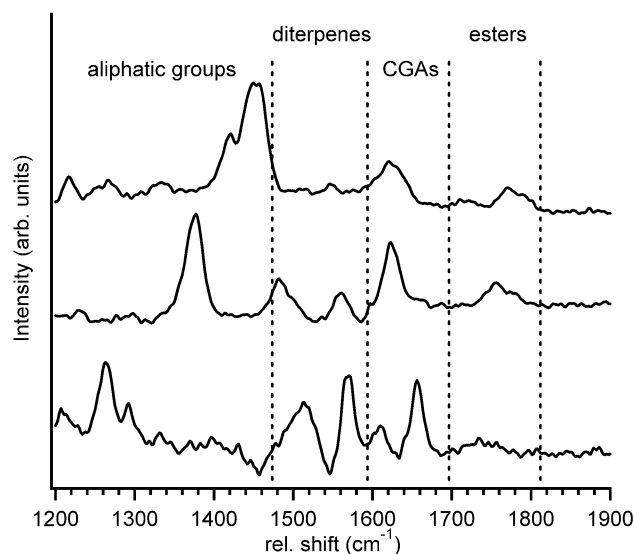


Figure 5. Typical Surface Enhanced Raman Spectra (SERS) of organic adsorbates measured from three individual Ag/CM particles optically trapped using a 532 nm laser.

These results indicate that organic adsorbates are indeed present at the Ag surface after synthesis of Ag/CM composites using coffee, and their presence is evident from the SERS signal obtained from trapped particles. Organic adsorbates appear to be strongly associated to the Ag surface given that their SERS spectrum persists after prolonged suspension in water (days); however they can be exchanged with ligands that strongly chemisorb as shown via SERS measurements using $Fe(CN)_6^{4-}$ solutions.

In summary, spectroscopic characterization using IRRAS and SERS together with TGA results indicate that organic compounds in coffee remain adsorbed at both the carbon and the metal nanoparticle surface when this natural reductant is used for the synthesis of composite microspheres.

Catalytic activity of composites

To investigate the catalytic activity of the Pd/CM composites we studied the hydrogenation of methyl-*trans*-cinnamate. The hydrogenation of methyl-*trans*-cinnamate is an ideal test reaction because high yields can be obtained in 2-3 h at room temperature under 1 atm of hydrogen.³³ The reactants are inexpensive and the products are relatively safe, *viz.* environmentally friendly. Given the facile nature of this reaction, it was deemed to be an acceptable standard to judge catalysts against.

Figure 6 shows the percent conversion from the hydrogenation of methyl-*trans*-cinnamate catalyzed by commercially available 10% Pd/activated carbon, Pd/CM and aPd/CM. Equal volumes of catalyst powder were used in all reactions. Each reaction was repeated in triplicate at each time interval. The average mass of palladium present in the 10% Pd/C reactions was 0.73 mg, while the Pd/CM and aPd/CM contained 0.06 mg and 0.03 mg palladium, respectively. From Figure 6 it is clear that reactions catalyzed by 10% Pd/C resulted in 100% conversion for all reactions ranging from 30 min to 120 min. Over the same reaction times, the Pd/CM produced results in the range of 0.2-1.3% conversion, with no observable trend. aPd/CM samples, which were not exposed to coffee solutions and therefore should display available palladium surface sites, yielded increased percent conversion vs. reaction time: after 30 min aPd/CM yielded $10 \pm 3\%$ conversion and by 120 min it yielded $92 \pm 17\%$ conversion. The 120 min conversion values are statistically indistinguishable from the conversion obtained with 10% Pd/C; however, this result is obtained with only 5% of the Pd mass compared to the commercial 10% Pd/C reactions and 50% of the Pd mass used in reactions run with Pd/CM as catalyst. Thus, this result demonstrates the impact that coffee residues have on the catalytic activity of the composites. When coffee is used in the synthesis, the biogenic corona is present, as shown above, blocking access to the palladium surfaces and the composites are not catalytically active. When coffee is not used in the synthesis, the nanoparticles surfaces are not blocked by a biogenic corona and the composites produce the same yields as commercially available catalysts albeit with 95% less metal.

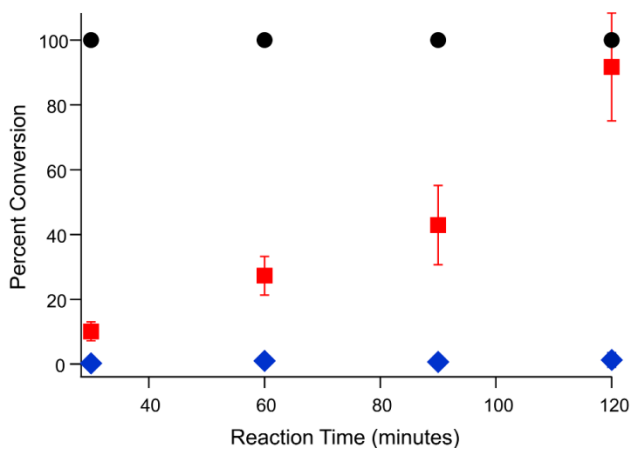


Figure 6. Percent conversion in the hydrogenation of methyl-*trans*-cinnamate reaction using Pd/CM (blue, diamonds), aPd/CM (red squares) and 10% Pd/C (black circles) catalysts.

Attempts were made to remove the coffee from the composites following synthesis. In one experiment the composites were washed 7 times, starting with deionized water, then using a mixture of water and ethanol, then ethanol. Each solvent was used until the supernatant was colorless. TGA analysis of the final product revealed that coffee was still present on the composites in the same concentrations as samples with fewer washing steps. Thus it appears that the coffee cannot be removed from the composite without strenuous effort or strong solvents, which would nullify any advantages arising from the use of greener synthesis. IRRAS results suggest that chlorogenic acids are preferentially adsorbed at the Pd surface; carboxylate groups are known to bind strongly to metals, resist multiple solvent washes and ultimately passivate surface sites. Thus, it is likely that the organic adlayer, or corona, which is present after reduction with coffee, cannot be easily removed post-synthesis. This problem is to be expected whenever complex natural extracts are used as green reductants in nanoparticle synthesis.

Conclusions

We investigated the surface chemistry of Ag/CM and Pd/CM composites produced using coffee as a natural reductant. Using SERS and IRRAS we demonstrated that organic constituents of coffee were present as adlayers on metal nanoparticle surfaces, while TGA measurements showed that organic

residues were also bound to the carbon microsphere scaffolds. Organic adsorbates form a corona that persists even after several washings and its impact on nanoparticle functionality was demonstrated through Pd-catalysed hydrogenation reactions. Using samples that were made with coffee, no reaction took place, however, Pd nanoparticles prepared on the same carbon supports without the use of coffee as a reductant yielded 100% reaction conversion, comparable to or better than a commercial Pd/C benchmark material.

These results demonstrate that the use of greener and/or more sustainable methods for nanomaterial synthesis does not necessarily yield nanomaterials with properties similar to those obtained with other synthetic techniques. They also validate the importance of performing careful chemical surface analysis of nanomaterials fabricated using greener and/or more sustainable methods. The biogenic corona that surrounds nanoparticles synthesized with natural reductants can dominate material functionality and affect its ultimate performance. Thus, if greener and/or more sustainable methods based on the use of natural compounds or biomass byproducts are to be adopted, the full utility of the materials they produce, which often hinges on their surface properties, must be quantified.

Acknowledgements. This work was supported by a grant from the Hewlett Mellon Fund for Faculty Development at Albion College (Michigan, USA). We are grateful to the Environmental Protection Agency (EPA) Ireland for financial support of this work through grant 2008-PhD-WRM-2. SERS work was carried out at the Central Laser Facility, STFC Rutherford Appleton Laboratory, supported through LSF Ref. No. 1192000. The authors are thankful to Dr. Clifford Harris at Albion College for his insightful suggestions.

Supporting Information Available. Raman spectra of single Ag/CM particles, SERS of nitrile stretching modes on Ag/CM particles. This material is available free of charge via the Internet at <http://pubs.acs.org>.

References

1. Mayer, K. M.; Hafner, J. H., Localized Surface Plasmon Resonance Sensors. *Chem. Rev.* **2011**, 111, 3828-3857.
2. Cao, Y. W. C.; Jin, R. C.; Mirkin, C. A., Nanoparticles with Raman spectroscopic fingerprints for DNA and RNA detection. *Science* **2002**, 297, 1536-1540.
3. Giljohann, D. A.; Seferos, D. S.; Daniel, W. L.; Massich, M. D.; Patel, P. C.; Mirkin, C. A., Gold Nanoparticles for Biology and Medicine. *Angew. Chem. Int. Ed* **2010**, 49, 3280-3294.
4. Jain, P. K.; Huang, X.; El-Sayed, I. H.; El-Sayed, M. A., Noble Metals on the Nanoscale: Optical and Photothermal Properties and Some Applications in Imaging, Sensing, Biology, and Medicine. *Acc. Chem. Res.* **2008**, 41, 1578-1586.
5. Somorjai, G. A.; Frei, H.; Park, J. Y., Advancing the Frontiers in Nanocatalysis, Biointerfaces, and Renewable Energy Conversion by Innovations of Surface Techniques. *J. Am. Chem. Soc.* **2009**, 131, 16589-16605.
6. Crooks, R. M.; Zhao, M. Q.; Sun, L.; Chechik, V.; Yeung, L. K., Dendrimer-encapsulated metal nanoparticles: Synthesis, characterization, and applications to catalysis. *Acc. Chem. Res.* **2001**, 34, 181-190.
7. Narayanan, R.; El-Sayed, M. A., Catalysis with transition metal nanoparticles in colloidal solution: Nanoparticle shape dependence and stability. *J. Phys. Chem. B* **2005**, 109, 12663-12676.
8. Astruc, D.; Lu, F.; Aranzaes, J. R., Nanoparticles as recyclable catalysts: The frontier between homogeneous and heterogeneous catalysis. *Angew. Chem. Int. Ed* **2005**, 44, 7852-7872.
9. Min, B. K.; Friend, C. M., Heterogeneous gold-based catalysis for green chemistry: Low-temperature CO oxidation and propene oxidation. *Chem. Rev.* **2007**, 107, 2709-2724.
10. Zhang, H.; Jin, M.; Xiong, Y.; Lim, B.; Xia, Y., Shape-Controlled Synthesis of Pd Nanocrystals and Their Catalytic Applications. *Acc. Chem. Res.* **2013**, 46, 1783-1794.
11. Kou, J.; Bennett-Stamper, C.; Varma, R. S., Green Synthesis of Noble Nanometals (Au, Pt, Pd) Using Glycerol under Microwave Irradiation Conditions. *ACS Sustain. Chem. Eng.* **2013**, 1, 810-816.
12. Kahrilas, G. A.; Wally, L. M.; Fredrick, S. J.; Hiskey, M.; Prieto, A. L.; Owens, J. E., Microwave-Assisted Green Synthesis of Silver Nanoparticles Using Orange Peel Extract. *ACS Sustain. Chem. Eng.* **2014**, 2, 367-376.
13. Akhtar, M. S.; Panwar, J.; Yun, Y.-S., Biogenic Synthesis of Metallic Nanoparticles by Plant Extracts. *ACS Sustain. Chem. Eng.* **2013**, 1, 591-602.
14. Nadagouda, M. N.; Varma, R. S., Green synthesis of silver and palladium nanoparticles at room temperature using coffee and tea extract. *Green Chem.* **2008**, 10, 859-862.
15. Nadagouda, M. N.; Iyanna, N.; Lalley, J.; Han, C.; Dionysiou, D. D.; Varma, R. S., Synthesis of Silver and Gold Nanoparticles Using Antioxidants from Blackberry, Blueberry, Pomegranate, and Turmeric Extracts. *ACS Sustain. Chem. Eng.* **2014**, 2, 1717-1723.

16. Baruwati, B.; Varma, R. S., High Value Products from Waste: Grape Pomace Extract-A Three-in-One Package for the Synthesis of Metal Nanoparticles. *Chemsuschem* **2009**, *2*, 1041-1044.
17. Markova, Z.; Novak, P.; Kaslik, J.; Plachtova, P.; Brazdova, M.; Jancula, D.; Siskova, K. M.; Machala, L.; Marsalek, B.; Zboril, R.; Varma, R., Iron(II,III)-Polyphenol Complex Nanoparticles Derived from Green Tea with Remarkable Ecotoxicological Impact. *ACS Sustain. Chem. Eng.* **2014**, *2*, 1674-1680.
18. Alam, M. N.; Roy, N.; Mandal, D.; Begum, N. A., Green chemistry for nanochemistry: exploring medicinal plants for the biogenic synthesis of metal NPs with fine-tuned properties. *RSC Advances* **2013**, *3*, 11935-11956.
19. Brumbaugh, A. D.; Cohen, K. A.; St Angelo, S. K., Ultrasmall Copper Nanoparticles Synthesized with a Plant Tea Reducing Agent. *ACS Sustain. Chem. Eng.* **2014**, *2*, 1933-1939.
20. Sintubin, L.; Verstraete, W.; Boon, N., Biologically produced nanosilver: Current state and future perspectives. *Biotechnol. Bioeng.* **2012**, *109*, 2422-2436.
21. Golinska, P.; Wypij, M.; Ingle, A.; Gupta, I.; Dahm, H.; Rai, M., Biogenic synthesis of metal nanoparticles from actinomycetes: biomedical applications and cytotoxicity. *Appl. Microbiol. Biotechnol.* **2014**, *98*, 8083-8097.
22. Mukherjee, P.; Ahmad, A.; Mandal, D.; Senapati, S.; Sainkar, S. R.; Khan, M. I.; Parishcha, R.; Ajaykumar, P. V.; Alam, M.; Kumar, R.; Sastry, M., Fungus-Mediated Synthesis of Silver Nanoparticles and Their Immobilization in the Mycelial Matrix: A Novel Biological Approach to Nanoparticle Synthesis. *Nano Lett.* **2001**, *1*, 515-519.
23. Dhillon, G. S.; Brar, S. K.; Kaur, S.; Verma, M., Green approach for nanoparticle biosynthesis by fungi: current trends and applications. *Crit. Rev. Biotechnol.* **2012**, *32*, 49-73.
24. Das, S. K.; Parandhaman, T.; Pentela, N.; Islam, A. K. M. M.; Mandal, A. B.; Mukherjee, M., Understanding the Biosynthesis and Catalytic Activity of Pd, Pt, and Ag Nanoparticles in Hydrogenation and Suzuki Coupling Reactions at the Nano-Bio Interface. *J. Phys. Chem. C* **2014**, *118*, 24623-24632.
25. Adil, S. F.; Assal, M. E.; Khan, M.; Al-Warthan, A.; Siddiqui, M. R. H.; Liz-Marzan, L. M., Biogenic synthesis of metallic nanoparticles and prospects toward green chemistry. *Dalton Trans.* **2015**, *44*, 9709-9717.
26. Ghodake, G.; Eom, C.-Y.; Kim, S. W.; Jin, E., Biogenic Nano-Synthesis; towards the Efficient Production of the Biocompatible Gold Nanoparticles. *Bull. Korean Chem. Soc.* **2010**, *31*, 2771-2775.
27. Punnoose, A.; Dodge, K.; Rasmussen, J. W.; Chess, J.; Wingett, D.; Anders, C., Cytotoxicity of ZnO Nanoparticles Can Be Tailored by Modifying Their Surface Structure: A Green Chemistry Approach for Safer Nanomaterials. *ACS Sustain. Chem. Eng.* **2014**, *2*, 1666-1673.
28. Duffy, P.; Reynolds, L. A.; Sanders, S. E.; Metz, K. M.; Colavita, P. E., Natural reducing agents for electroless nanoparticle deposition: Mild synthesis of metal/carbon nanostructured microspheres. *Mater. Chem. Phys.* **2013**, *140*, 343-349.
29. Esquivel, P.; Jiménez, V. M., Functional properties of coffee and coffee by-products. *Food Res. Int.* **2012**, *46*, 488-495.

30. Duffy, P.; Magno, L. M.; Yadav, R. B.; Roberts, S. K.; Ward, A. D.; Botchway, S. W.; Colavita, P. E.; Quinn, S. J., Incandescent porous carbon microspheres to light up cells: solution phenomena and cellular uptake. *J. Mater. Chem.* **2012**, *22*, 432-439.
31. Gazi, E.; Ward, A. D.; Clarke, N. W.; Harvey, T. J.; Snook, R. D.; Gardner, P.; Faria, E. C.; Brown, M. D.; Henderson, A., Spectral discrimination of live prostate and bladder cancer cell lines using Raman optical tweezers. *J. Biomed. Opt.* **2008**, *13*, 064004.
32. Sanderson, J. M.; Ward, A. D., Analysis of liposomal membrane composition using Raman tweezers. *Chem. Commun.* **2004**, 1120-1121.
33. O'Connor, K. J.; Zuspan, K.; Berry, L., An Undergraduate Organic Chemistry Laboratory: The Facile Hydrogenation of Methyl trans-Cinnamate. *J. Chem. Educ.* **2010**, *88*, 325-327.
34. Skrabalak, S. E.; Suslick, K. S., Porous Carbon Powders Prepared by Ultrasonic Spray Pyrolysis. *J. Am. Chem. Soc.* **2006**, *128*, 12642-12643.
35. Skrabalak, S. E.; Suslick, K. S., Carbon powders prepared by ultrasonic spray pyrolysis of substituted alkali Benzoates. *J. Phys. Chem. C* **2007**, *111*, 17807-17811.
36. Ferrari, A. C.; Robertson, J., Interpretation of Raman spectra of disordered and amorphous carbon. *Phys. Rev. B* **2000**, *61*, 14095-14107.
37. Akhter, M. S.; Chughtai, A. R.; Smith, D. M., The structure of hexanesoot- I - Spectroscopic studies. *Appl. Spectrosc.* **1985**, *39*, 143-153.
38. Smith, D. M.; Chughtai, A. R., The surface structure and reactivity of black carbon. *Colloids Surf. A* **1995**, *105*, 47-77.
39. Socrates, G., *Infrared and Raman Characteristic Group Frequencies: Tables and Charts*. 3rd ed.; John Wiley & Sons, LTD.: New York, 2001.
40. Metz, K. M.; Colavita, P. E.; Tse, K.-Y.; Hamers, R. J., Nanotextured gold coatings on carbon nanofiber scaffolds as ultrahigh surface-area electrodes. *J. Power Sources* **2012**, *198*, 393-401.
41. Shter, G. E.; Shindler, Y.; Matatov-Meytal, Y.; Grader, G. S.; Sheintuch, M., Thermal behavior of the phenol-Pd-ACC system. *Carbon* **2002**, *40*, 2547-2557.
42. Zhang, H.; Gromek, J.; Fernando, G. W.; Boorse, S.; Marcus, H. L., PdO/Pd system equilibrium phase diagram under a gas mixture of oxygen and nitrogen. *J. Phase Equilib.* **2002**, *23*, 246-248.
43. Lyman, D. J.; Benck, R.; Dell, S.; Merle, S.; Murray-Wijelath, J., FTIR-ATR Analysis of Brewed Coffee: Effect of Roasting Conditions. *J. Agric. Food Chem.* **2003**, *51*, 3268-3272.
44. Briandet, R.; Kemsley, E. K.; Wilson, R. H., Discrimination of Arabica and Robusta in Instant Coffee by Fourier Transform Infrared Spectroscopy and Chemometrics. *J. Agric. Food Chem.* **1996**, *44*, 170-174.
45. Wang, N.; Lim, L.-T., Fourier Transform Infrared and Physicochemical Analyses of Roasted Coffee. *J. Agric. Food Chem.* **2012**, *60*, 5446-5453.

46. Wermelinger, T.; D'Ambrosio, L.; Klopprogge, B.; Yeretjian, C., Quantification of the Robusta Fraction in a Coffee Blend via Raman Spectroscopy: Proof of Principle. *J. Agric. Food Chem.* **2011**, *59*, 9074-9079.
47. Keidel, A.; von Stetten, D.; Rodrigues, C.; Máguas, C.; Hildebrandt, P., Discrimination of Green Arabica and Robusta Coffee Beans by Raman Spectroscopy. *J. Agric. Food Chem.* **2010**, *58*, 11187-11192.
48. Rubayiza, A. B.; Meurens, M., Chemical Discrimination of Arabica and Robusta Coffees by Fourier Transform Raman Spectroscopy. *J. Agric. Food Chem.* **2005**, *53*, 4654-4659.
49. Loo, B. H.; Lee, Y. G.; Liang, E. J.; Kiefer, W., Surface-enhanced Raman scattering from ferrocyanide and ferricyanide ions adsorbed on silver and copper colloids. *Chem. Phys. Lett.* **1998**, *297*, 83-89.

Figure 1. (a) SEM image of bare carbon microspheres synthesized from potassium dichloroacetate precursor solutions; (b) Size distribution of carbon microspheres; (c) Raman of carbon microspheres measured from the dry powder, excitation 457 nm; (d) FTIR absorbance spectrum of carbon microspheres.

Scheme 1. Synthesis protocol used for the preparation of Pd/CM materials.

Figure 2. SEM image showing details of the carbon scaffold walls after (a) sensitization with Sn^{2+} , (b) activation with PdCl_4^{2-} and (c) coffee reduction.

Figure 3. TGA curves obtained at $10\text{ }^\circ\text{C min}^{-1}$ in air for: (a) bare carbon microspheres (CM, black solid line), activated palladium on CM (aPd/CM, red dotted line) and palladium nanoparticles on carbon microspheres (Pd/CM, blue dashed line); (b) bare carbon microspheres (CM, black solid line) and carbon microspheres after incubation in coffee (red dashed line).

Figure 4. IRRAS spectrum of a Pd surface after exposure to coffee, obtained using a bare Pd substrate as the background sample (bottom, red trace) and ATR-FTIR spectrum of coffee powder (top black trace). Spectra were baseline corrected and offset for clarity; the coffee powder spectrum was multiplied by 0.1 to facilitate comparison.

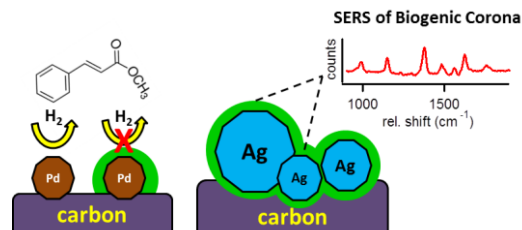
Figure 5. Typical Surface Enhanced Raman Spectra (SERS) of organic adsorbates measured from three individual Ag/CM particles optically trapped using a 532 nm laser.

Figure 6. Percent conversion of reactions run using Pd/CM (blue, diamonds), aPd/CM (red squares) and 10% Pd/C (black circles) catalysts.

For Table of Contents Use Only

Green synthesis of metal nanoparticles via natural extracts: the biogenic nanoparticle corona and its effects on reactivity

Kevin M. Metz, Stephanie E. Sanders, Joshua P. Pender, Michael R. Dix, David T. Hinds, Susan J. Quinn, Andrew D. Ward, Paul Duffy, Ronan J. Cullen, and Paula E. Colavita



This work investigates the composition and effects of the biogenic corona present at Ag and Pd nanoparticles after synthesis via green methodologies.